The synergistic effects between Ce and Cu in $Cu_yCe_{1-y}W_5O_x$ catalysts for enhanced NH_3-SCR of NO_x and SO_2 tolerance

Jian-Wen Shi[a,*], Yao Wang[a], Ruibin Duan[b], Chen Gao[a], Baorui Wang[a], Chi He[c,*], Chunming Niu[a]

[a] *State Key Laboratory of Electrical insulation and Power Equipment, Center of Nanomaterials for Renewable Energy, School of Electrical Engineering, Xi'an Jiaotong University, Xi'an 710049, China.*

[b]*Guangdong Provincial Academy of Building Research Group Co., Ltd., Guangzhou 510530, China*

[c]*Department of Environmental Science and Engineering, School of Energy and Power Engineering, Xi'an Jiaotong University, Xi'an 710049, China*

Corresponding author:

Jian-Wen Shi, E-mail: jianwen.shi@mail.xjtu.edu.cn

Chi He, E-mail: chi_he@xjtu.edu.cn

Figures and Tables

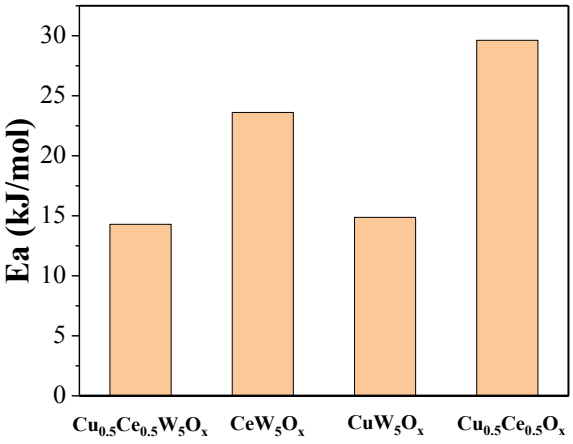

Fig. S1 The apparent activation energies of the catalysts.

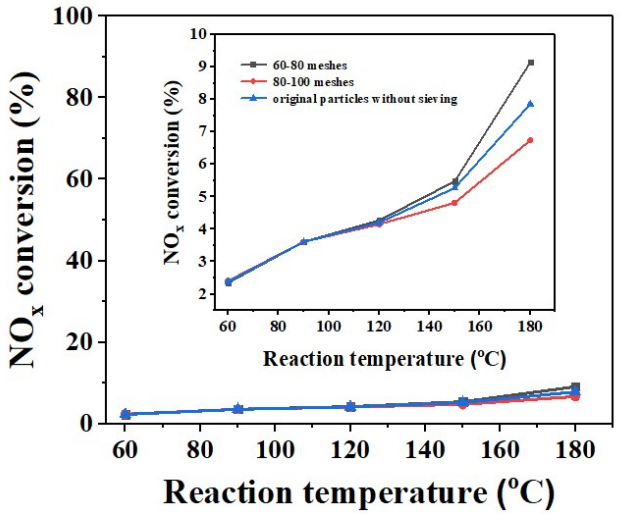

Fig. S2 The NO_x conversions as a function of temperature over the $Cu_{0.5}Ce_{0.5}W_5O_x$ catalyst with different pellet particle sizes (60-80 and 80-100 meshes by sieving, and the original catalysts without sieving, respectively) under the GHSV of 216,000 h^{-1}.

In order to further ensure the reaction was in the kinetic regime, the SCR de-NOx performance of the $Cu_{0.5}Ce_{0.5}W_5O_x$ catalyst was further evaluated under a higher GHSV of 216,000 h^{-1}, and three $Cu_{0.5}Ce_{0.5}W_5O_x$ catalysts with different particle sizes were utilized to measure the possible mass-transfer limitation (60-80 and 80-100 meshes by sieving, and the original catalysts without sieving, respectively). As shown in Fig. S4, under such a high GHSV of 216,000 h-1, the NO_x conversions at all temperature points were below 10%, so the reaction was in the kinetic regime. From the inset in Fig. S4, it can be seen that a slight difference can be identified among the three catalysts when the scale of Y-axis was set to 2-10, but the slight difference can be ignored when the scale of Y-axis was set to 0-100, indicating the affection of mass transport limitation can be nearly excluded.

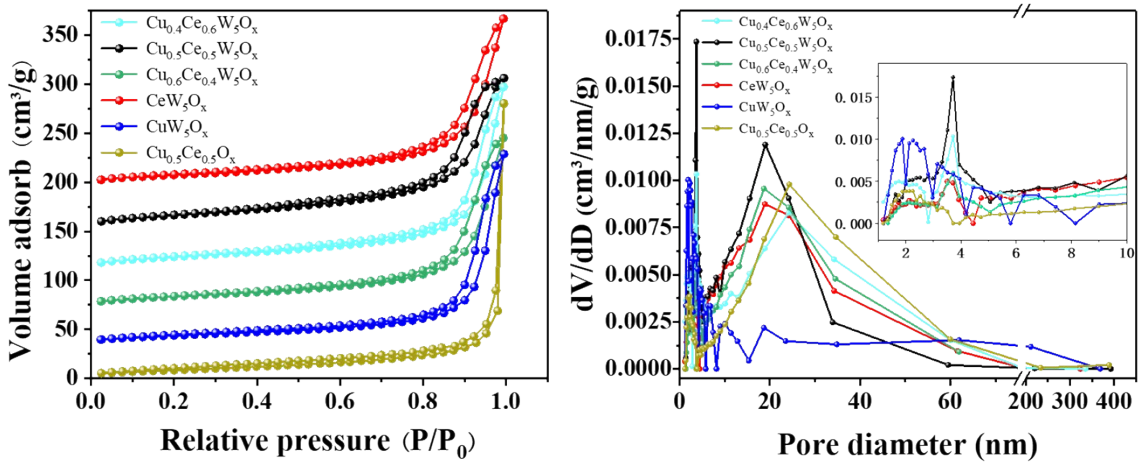

Fig. S3 Nitrogen adsorption and desorption isothermals (A, left) and pore size distributions (B, right) of all catalysts.

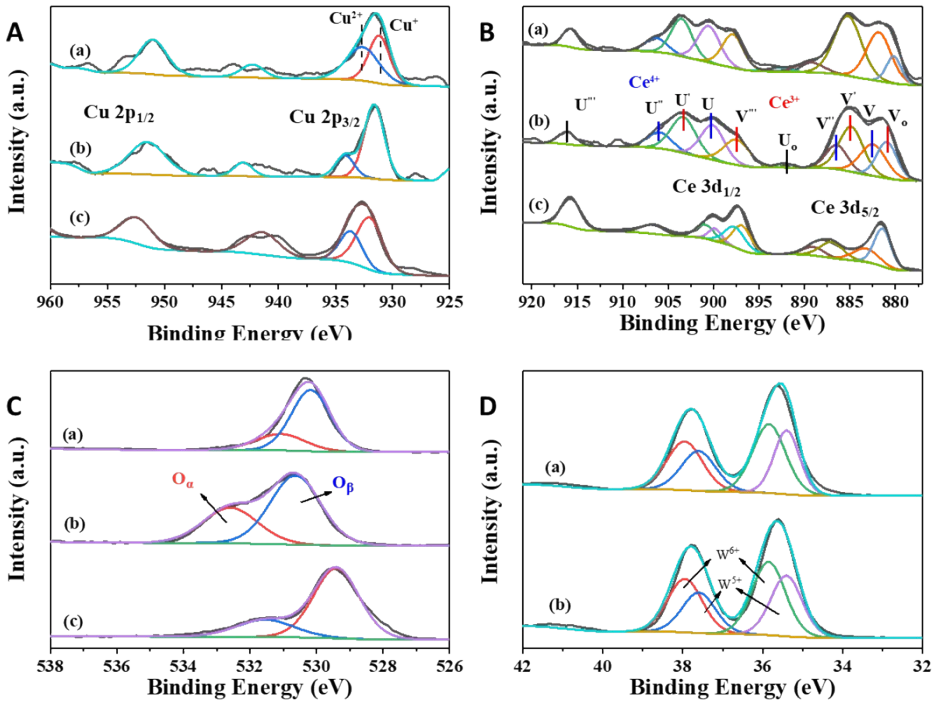

Fig. S4 The high-resolution XPS spectra of Cu2p (A), Ce3d (B), O1s (C) and W4f (D): (a) $Cu_{0.4}Ce_{0.6}W_5O_x$, (b) $Cu_{0.6}Ce_{0.4}W_5O_x$, (c) $Cu_{0.5}Ce_{0.5}O_x$.

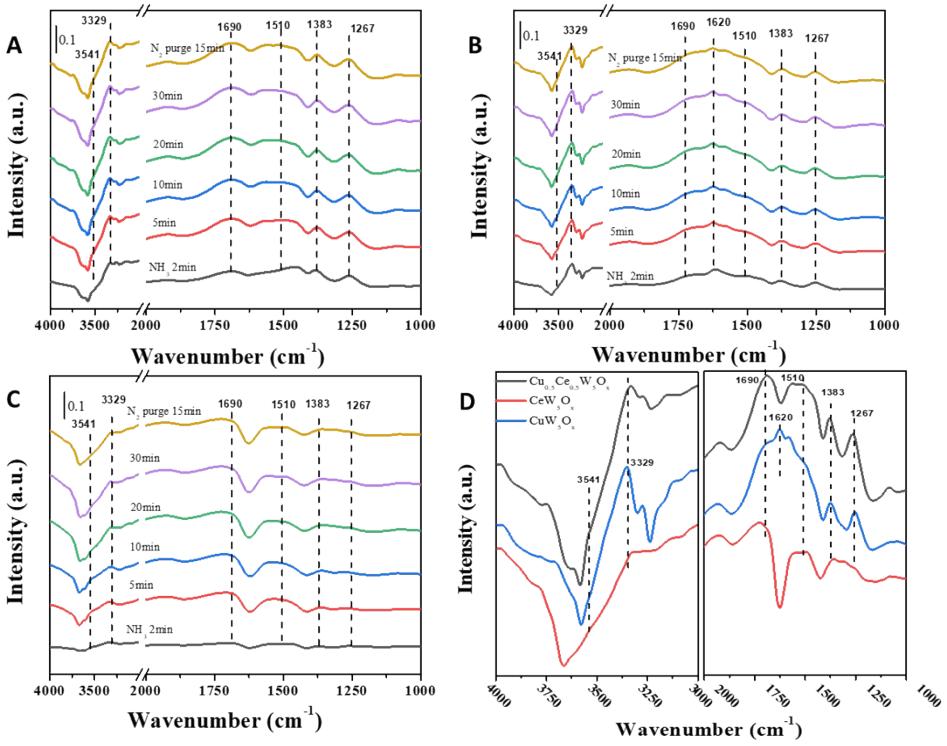

Fig. S5 In-situ DRIFT spectra of NH_3 adsorption at 210 °C over $Cu_{0.5}Ce_{0.5}W_5O_x$ (A), CuW_5O_x (B) and CeW_5O_x (C) for 2, 5, 10, 15, 30 min and N_2 purge for 15 min, and the comparison of the in-situ DRIFT spectra over $Cu_{0.5}Ce_{0.5}W_5O_x$, CuW_5O_x and CeW_5O_x after N_2 purge for 15 min (D).

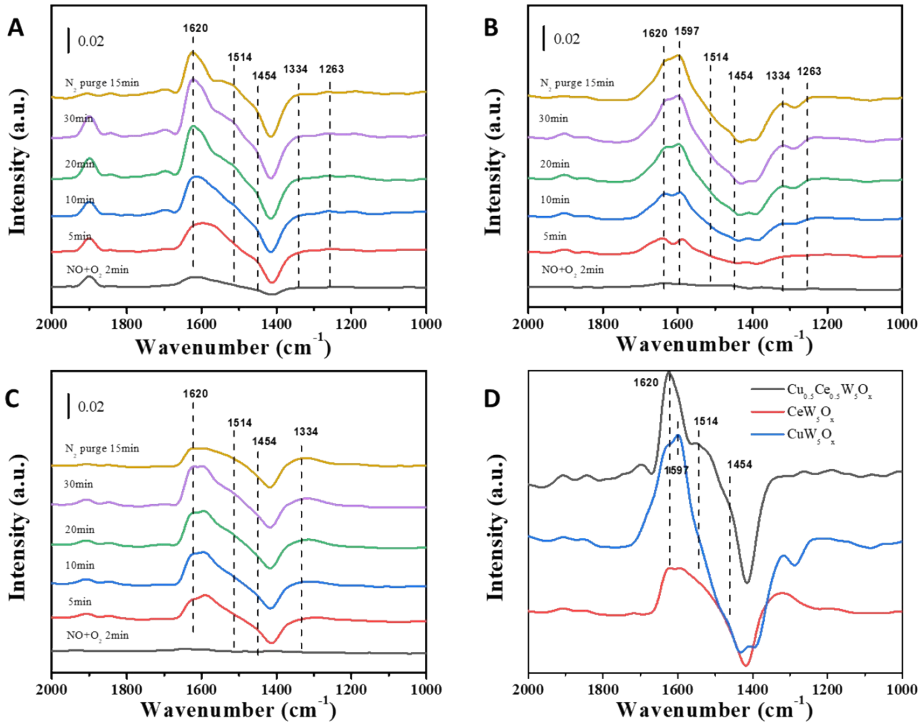

Fig. S6 In-situ DRIFT spectra of $NO+O_2$ adsorption at 210 °C over $Cu_{0.5}Ce_{0.5}W_5O_x$ (A), CuW_5O_x (B) and CeW_5O_x (C) for 2, 5, 10, 15, 30 min and N_2 purge for 15 min, and the comparison of the in-situ DRIFT spectra over $Cu_{0.5}Ce_{0.5}W_5O_x$, CuW_5O_x and CeW_5O_x after N_2 purge for 15 min (D).

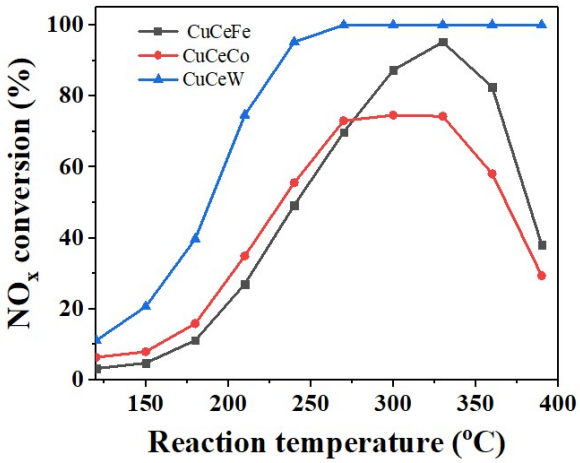

Fig. S7 The comparison of de-NO_x performances over three catalysts, the CuCeW, CuCeFe and CuCeCo (reaction conditions: 500 ppm NO, 500 ppm NH_3, 5 vol.% O_2, balanced with N_2, GHSV = 36,000 h^{-1}).

Table S1. Summary and comparison on the SO_2 tolerance of this work and other literature.

Catalyst	Reaction conditions	X_{NO}	X_{NO}-U	X_{NO}-A	Ref.
Cu-Ce-W	0.05%NH_3, 0.05%NO, 5%O_2, 50 ppm SO_2, 36000 h^{-1}, 240 ^oC	95%	60%	64%	This work
Mn/TiO_2	0.06%NH_3, 0.06%NO, 5%O_2, 50 ppm SO_2, 108000 h^{-1}, 150 ^oC	79%	54%	68%	29
MnNb/TiO	0.06%NH_3, 0.06%NO, 5%O_2, 50 ppm SO_2, 108000 h^{-1}, 150 ^oC	90%	80%	86%	29
CrOx/C	0.05%NH_3, 0.05%NO, 5%O_2, 50 ppm SO_2, 30000 h^{-1}, 150 ^oC	95%	60%	~	30
MnCe/TNT	0.07%NH_3, 0.07%NO, 3.5%O_2, 250 ppm SO_2, 100000 h^{-1}, 300 ^oC	93%	83%	89%	31
$MnCe/TiO_2$	0.07%NH_3, 0.07%NO, 3.5%O_2, 250 ppm SO_2, 100000 h^{-1}, 300 ^oC	70%	51%	64%	31
MnCe	0.05%NH_3, 0.05%NO, 5%O_2, 150 ppm SO_2, 48000 h^{-1}, 175 ^oC	87%	60%	73%	32
MgMnCe	0.05%NH_3, 0.05%NO, 5%O_2, 150 ppm SO_2, 48000 h^{-1}, 175 ^oC	98%	70%	84%	32
FeMn/TiZr	0.1%NH_3, 0.1%NO, 3%O_2, 100ppm SO_2, 30000 h^{-1}, 150 ^oC	91%	44%	~	33
MnCe/Ti	0.08%NH_3, 0.08%NO, 3%O_2, 100 ppm SO_2, 40000 h^{-1}, 150 ^oC	100%	62%	~	34
Mn/Ti	0.08%NH_3, 0.08%NO, 3%O_2, 100 ppm SO_2, 40000 h^{-1}, 150 ^oC	92%	27%	~	34

X_{NO}, X_{NO}-U, and X_{NO}-A represent NO_x conversion of regular SCR reaction, NO_x conversion under the tolerance test and after tolerance test, respectively.

Table S2. Summary of the results on non-manganese-based catalysts in literature.

Catalyst	Preparation method	Heat-treatment conditions	Reaction conditions	The best NO_x conversion	Ref.
Cu-Ce-W	Co-precipitation	400 °C/4h	0.05%NH_3, 0.05%NO, 5%O_2, 100000 h^{-1}	100% (270~390 °C)	This work
Ce-Mo-Ti	Impregnation method	500 °C/4h	0.05%NH_3, 0.05%NO, 3%O_2, 71000 h^{-1}	100% (300~400 °C)	21
Ce-W/Ti-Si	Co-precipitation	500 °C/5h	0.05%NH_3, 0.05%NO, 3%O_2, 30000 h^{-1}	100% (250~400 °C)	22
Cu-W-Zr	Co-precipitation	500 °C/3h	0.05%NH_3, 0.05%NO, 5%O_2, 30000 h^{-1}	95% (225~300 °C)	31
Cu-Ce	Citric acid method	350 °C/5h	0.06%NH_3, 0.06%NO, 5%O_2, 28000 h^{-1}	95% (180~210 °C)	32
Cu-Ce-Zr	Citric acid method	500 °C/5h	0.1%NH_3, 0.1%NO, 3%O_2, 28000 h^{-1}	100% (180~240 °C)	33
Cu-Ce	Co-precipitation	350 °C/3h	0.1%NH_3, 0.1%NO, 5%O_2, 40000 h^{-1}	98% (250~350 °C)	34
Ce-ACFN	Impregnation method	350 °C/6h	0.1%NH_3, 0.1%NO, 5%O_2, 11000 h^{-1}	95% (150~270 °C)	35
Fe-Ti	Co-precipitation	550 °C/3h	0.05%NH_3, 0.05%NO, 2%O_2, 120000 h^{-1}	100% (350~400 °C)	36
Cu-Fe-Ti	Sol-gel method	500 °C/3h	0.05%NH_3, 0.05%NO, 3.5%O_2, 60000 h^{-1}	90% (200~250 °C)	37
Co-Fe-Ti	Sol-gel method	500 °C/3h	0.05%NH_3, 0.05%NO, 3.5%O_2, 60000 h^{-1}	95% (225 °C)	37
Fe-Co	Hydrothermal method	700 °C/4h	0.2%CO, 0.1%NO, 3.5%O_2, 6000 h^{-1}	100% (200~350 °C)	38
Ce-W	Hydrothermal method	400 °C/4h	0.05%NH_3, 0.05%NO, 3%O_2, 300000 h^{-1}	80% (300 °C)	39
Fe-W	Stepwise urea-assisted method	500 °C/5h	0.05%NH_3, 0.05%NO, 3%O_2, 300000 h^{-1}	98% (250~400 °C)	40

Table S3. Structural parameters and E_a (kJ mol^{-1}) of the catalysts.

Catalyst	S_{BET} (m^2/g)	Pore volume (cm^3/g)	Pore diameter (nm)	E_a (kJ mol^{-1})	Curve area (normalize) NH_3-TPD	NO-TPD
$Cu_{0.4}Ce_{0.6}W_5O_x$	55.3	0.30	3.72	/	1.69	1.43
$Cu_{0.5}Ce_{0.5}W_5O_x$	**64.7**	0.25	3.72	**14.29**	**1.71**	**1.64**
$Cu_{0.6}Ce_{0.4}W_5O_x$	53.9	0.28	18.68	/	1.29	1
CeW_5O_x	55.5	0.27	18.88	23.61	1	1.43
CuW_5O_x	44.4	0.31	24.32	14.87	1.40	1.10
$Cu_{0.5}Ce_{0.5}O_x$	26.9	0.44	1.88	29.62	/	/

Table S4. Relative atomic concentration on the surface of the three catalysts.

Catalyst	Surface atomic concentrations (%)				Relative concentration ratios (%)			
	Cu	Ce	W	O	Cu^{2+}/Cu	Ce^{3+}/Ce	W^{5+}/W	O_a/O
$Cu_{0.5}Ce_{0.5}W_5O_x$	2.24	3.40	22.93	47.64	28.57	39.3	60.4	38.6
CeW_5O_x	/	4.34	19.53	41.93	/	29.5	43.6	32.0
CuW_5O_x	3.37	/	18.58	44.10	31.51	/	26.2	24.2

Table S5 The atomic concentration of the $Cu_yCe_{1-y}W_5O_x$ catalysts

Sample	Cu (%)	Ce (%)	W (%)	O (%)	Cu/Ce
$Cu_{0.4}Ce_{0.6}W_5O_x$	0.60	1.18	47.57	50.66	0.51
$Cu_{0.5}Ce_{0.5}W_5O_x$	1.41	1.70	40.85	56.04	0.83
$Cu_{0.6}Ce_{0.4}W_5O_x$	0.67	0.44	48.65	50.24	1.52